Roy and Das
Journal of Engineering and Applied Science (2023) 70:110
https://doi.org/10.1186/s44147-023-00287-5

Journal of Engineering and Applied Science

RESEARCH Open Access

A modified decomposition method for the analysis of porous triangular fin with a power exponent of thermal properties and magnetic effect

Pranab Kanti Roy[1*] and Joy Prakash Das[2]

*Correspondence:
pranab38_skd@yahoo.com

[1] Department of Mechanical Engineering, Seacom Skills University, Kendradangal, Birbhum, West Bengal 731236, India
[2] Department of Mathematics, Seacom Skills University, Kendradangal, Birbhum, West Bengal 731236, India

Abstract

A closed-form solution of the triangular porous fin with a simultaneous variation of power law-dependent heat transfer coefficient, internal heat generation, and surface emissivity parameters under the influence of external magnetic and electric fields is carried out. Darcy's model has been used to simulate flow in the porous triangular fin with insulated boundary conditions. The governing singular value equation is nondimensionalized and solved by modified Adomian decomposition method (MADM) and the results of MADM are compared with the numerical solution obtained from the finite difference method (FDM) in the limiting conditions. The graphical analysis of the significant power law variation of thermophysical parameters, Hartmann number and important design parameters such as the half-thickness parameter of the triangular fin are performed and physically interpreted. A comparative study has been carried out with multiple power law parameters at different values while other thermophysical parameters were kept at a fixed level and it has been found that fin temperature is highest at higher values of power index parameters. From this study, it has been found that with the increasing value of the Hartmann number as well as the porosity parameter, the efficiency of the triangular porous fin increases rapidly.

Keywords: Variable area, Porosity, Magnetic effect, Modified differential operator

Introduction

Fin has a central role in core thermal engineering applications where they are used to increase the energy transfer from the solid wall to the environment. The various profiles of fins are available depending on the application. They are selected on the basis of the economy of materials and production with consideration of the fabrication process. In perspective to the content of design and fabrication, the rectangular shapes of fins are considered as basic geometry and it has a wide application for example, in the electronics industry, automobile industry, and many other [1–3]. This attempt highlights in application of fin where weight is not the major criterion. However, the utilization of materials and lightweight is the prime factor in some of the applications such as for

space applications and therefore research works on various fin profiles, such as convex/concave, exponential, and triangular profiles are the interest of current research. The triangular profile is attractive due to reduced volume for the same heat transfer rate as compared to the rectangular profile and is easy to manufacture due to its straight edge as compared to the other curved profile. A vast review related to the fins is presented by Kraus [4].

For the last two decades, in the perspective of quick heat dissipation from the fin surface, researchers have increased their interest in the heat transfer study of porous fin. The mechanism of increasing the heat transfer rate is to increase the effective surface area, which is made by interconnected voids that increase the convective-radiative heat dissipation from the surface. The earlier research works focused on a different role of involved operating parameters and their thermal performance on the porous surface in order to implement such application [5, 6]. Kiwan and Al-Nimr [7] studied numerically porous fins for increasing heat transfer for certain porosity parameter with different design and operating conditions. Kiwan [8] investigated porous fins under a natural convection environment. Gorla and Bakier [9] studied longitudinal rectangular porous fins with a combined mode of both convection and radiation in which Darchy's model is used for interaction between solid and fluid interaction. They proved mathematically that porous fins have better heat transfer characteristics as compared to solid fins. Kundu and Bhanja [10] presented the performance and optimization of the longitudinal porous fin with different mathematical models. Constructal T-shape porous fin with convection and radiation effects for different geometric and thermo-physical parameters are also investigated by Kundu and Bhanja [11]. An increased heat transfer performance is observed in this type of fin for choosing the porous medium.

For solving the problem of extended surfaces with porous medium, many solution methodologies are available for solving non-linear problems. Further singularity in the governing equation in conjunction with the non-linearity introduces additional complexity. Some of the methods such as the differential transfer method (DTM) can be implemented for solving non-linear problems with both singularity and non-singularity. Moradi et al. [12] investigated triangular porous fin where energy balance includes conduction accompanied by Rossland's radiation law from the fin's base and convection with Stephen's Boltzmann's radiation from the fin's surface with temperature variation of thermal conductivity. The singular and non-linear equation is solved by DTM analytically and Runge–Kutta fourth order method is used for numerical study and both methods revealed a good agreement. The same DTM along with other approximation methods namely collocation method [CM], and least square method [LSM] are used to solve the non-singular type energy equation of rectangular profile with Si3N4 and Al materials by Hatami et al. [13]. Oguntala et al. [14] applied another approximate analytical method proposed by Daftardar–Gejiji and Jafari Method (DJM) for the analysis of the non-singular energy equation of constant cross-section of the porous fin. The results of DJM are in good agreement with the fourth-order Runge–Kutta method. Some methodology fails to deal with singular value problem whereas others are suitable for non-singular value problem. In that perspective to analyze the fin problem, Roy et al. [15] have selected two categories of fins, one with constant cross-section and the other with varying cross-section with several thermo-physical parameters function of temperature. The theory of the classical Adomian decomposition method (ADM)

has been carried out to resolve the multiple non-linearity of the rectangular energy equation. The energy equations of convex and triangular fins with the same non-linearity have a behavior of singularity and therefore the concept of modified Adomian decomposition theory (MADM) has been carried out and their all results revealed a good agreement with the exact solution [15]. Similarly, the same concept of classical and modified decomposed solution was obtained for heat transfer analysis of rectangular, convex, and triangular cross-section absorber plate solar collectors with power law-dependent thermal properties [16].

Many studies on fins with multiple temperature dependence relations have attracted many researchers in which majority of the cases they considered the coefficient of heat transfer as power law and other thermo-physical parameters as linear or sometimes quadratic/polynomial law. This is due to the fact that in several industrial processes, the values of power indices of heat transfer coefficient indicates specific heat transfer process, for example when the numerical value of n is -0.25, it is called condensation or laminar film boiling, 0.25 it is laminar natural convection, and 2 for nucleate boiling. This power index analogy can be extended for other parameters in order to intensify the aforementioned heat transfer process and bring the variation to one mathematical platform. Mosayebidorcheh et al. [17] and Moitsheki et al. [18] with separate mathematical techniques investigated rectangular fins, and the variation of the power law concept is applied equally both for thermal conductivity and heat transfer coefficient. The same is extended for variable cross-sections such as convex and concave profile [19].

Although, the porous fin is widely accepted and has interconnected voids in order to flow the gas particles through the passage, additionally applied electric and magnetic field ionizes the gas particles and enhances additional velocity which leads to the increased heat transfer rate. Sobamowo [20], Das and Kundu [21], Hoshyar, et al. [22], and Patel and Meher [23] investigated the longitudinal porous fin with electric and magnetic fields. Gireesha et al. [24] studied the radial porous fin numerically where they assumed only heat transfer co-efficient as a power law. Madhura et al. [25] investigated straight rectangular porous fins with variable thermal conductivity. Das and Kundu [26] investigated forward and inverse heat transfer study of longitudinal porous fin numerically using magnetic field for electronic cooling.

On the aforementioned literature survey, it is clear that there is no work available in the literature in the case of porous triangular fin in which the researcher investigated the multiple variations of thermophysical parameters. Therefore, in the current work, an attempt has been made to bring the variation of all thermo-physical parameters into one mathematical platform in order to predict the heat transfer process correctly. Additionally, it has been observed that the application of an external magnetic field enhances the rate of heat transfer process in the porous fin. Considering the above research gap to the author's knowledge, the present research work has been undertaken to study the multiple variations of the thermophysical parameter as power law dependent on the application of the external magnetic effect.

Methods

The objective of the present study is to obtain closed-form solutions of the triangular porous fin with multiple power law-dependent thermal properties. Darcy's equation is used to formulate the flow of fluids through a porous medium where the flow of fluids is

influenced by external electric and magnetic fields. The energy equation of a triangular fin with insulated boundary conditions is a singular non-linear type equation. The MADM has been employed to solve the singular non-linear type equation and the results of MADM are compared with the finite difference method (FDM) in the limiting condition.

Mathematical formulation of the physical problem

Figure 1a shows the physical feature of a triangular cross-section longitudinal porous fin whose base is affixed to a plate of constant temperature. For simplicity of the problem, a few assumptions are considered below.

- ➢ The medium is to be isotropic and homogeneous and saturated fluid without phase change although a uniform magnetic field is applied.
- ➢ The concept of local thermal equilibrium of both fluid and porous medium is applied in the domain.
- ➢ The steady with one-dimensional model is assumed.
- ➢ To simulate the fluid particles in the domain Darcy's model is engaged.
- ➢ A uniform magnetic field is applied vertically and temperature is a function of x only.

The energy equation for the differential element at a location x from the tip of the porous fin as

$$\frac{dq_x}{dx}dx + q(t)A_x dx = h(t)P_x(1-\varphi)(T-T_a) + \dot{m}C_m(T-T_a) + \sigma\varepsilon(t)P_x dx\left(T^4 - \frac{\alpha}{\varepsilon_s}T_a^4\right) + \frac{J_c \times J_c}{\sigma_m}dx \tag{1}$$

where A_x is area P_x perimeter at the location x. For solving the Eq. (1), two boundary conditions are required as follows:

$$At\ tip\ :\qquad T(x)]_{x=0} = 0 \tag{2a}$$

$$At\ base\ :\qquad T(x)]_{X=L} = T_b \tag{2b}$$

The power law variations of thermophysical parameters are applied as follows:

$$h(T) = h_b\left(\frac{T-T_a}{T_b-T_a}\right)^n \tag{3a}$$

$$\varepsilon(T) = \varepsilon_s\left(\frac{T-T_a}{T_b-T_a}\right)^B \tag{3b}$$

$$q(T) = q_0\left(\frac{T-T_a}{T_b-T_a}\right)^{\varepsilon_G} \tag{3c}$$

Using the similarity law from the geometrical relationship of the fin in the vertical plane as shown in Fig. 1b,

$$\frac{dy}{dx} = \frac{y_b}{L} \text{ and } \frac{y}{x} = \frac{y_b}{L}$$

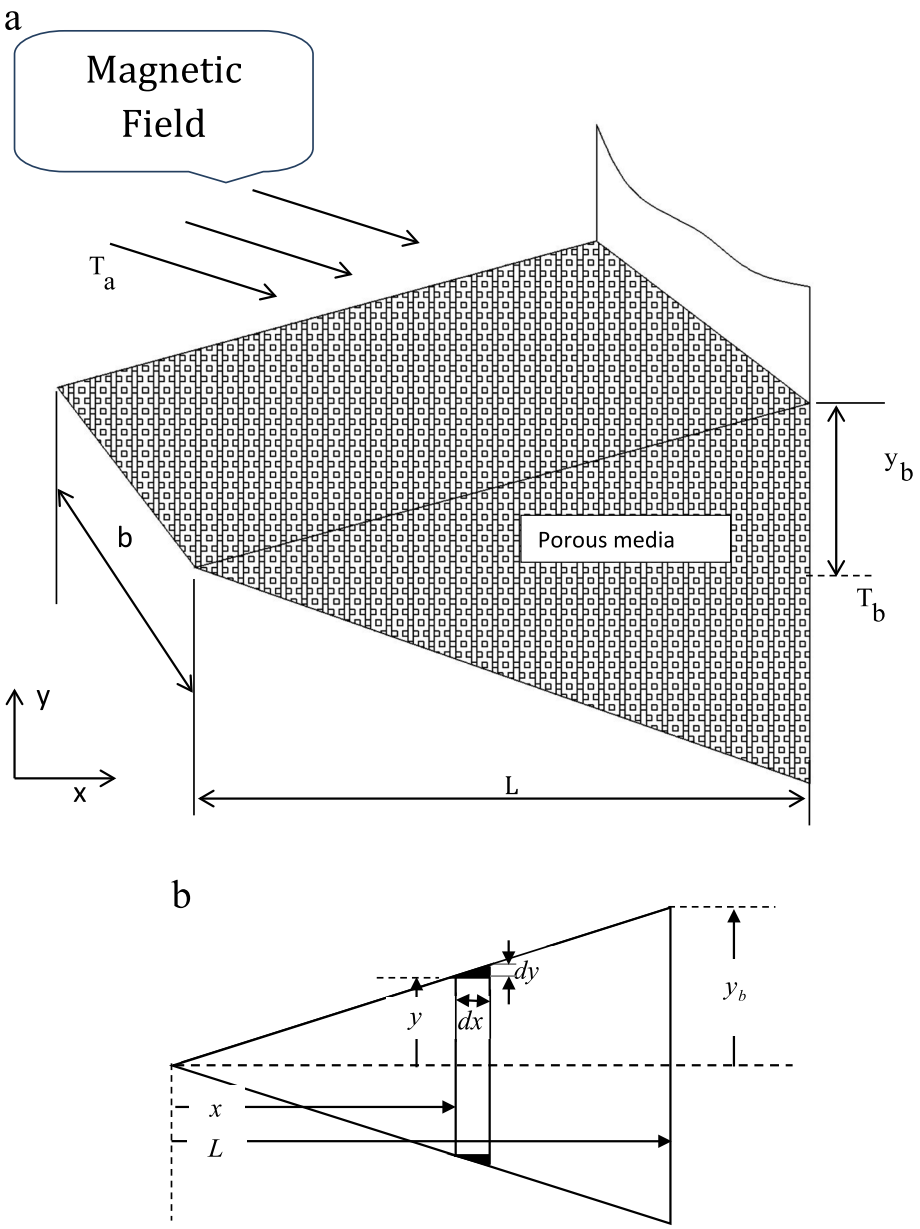

Fig. 1 **a** Important feature of triangular cross-section porous fin in three dimensions. **b** Physical coordinates of triangular porous fin in vertical plane

Since vertical distance y is the linear function of x, therefore cross-sectional area A_x and perimeter P_x for the triangular fin from tip to base is calculated as follows:

$$A_x = 2 \times \frac{y}{2} b = \left(\frac{x}{L}\right) y_b b \tag{4}$$

$$P_x = (2y + b)\sqrt{1 + \left(\frac{dy}{dx}\right)^2} \tag{5}$$

The mass flow rate $\dot{m}$ and Darcy's velocity related by the relation $\dot{m} = \rho V_W (2y + b)\sqrt{1 + \left(\frac{dy}{dx}\right)^2}\,dx$. The cross product of current density produces the magnetic field in the porous media and it can be related as follows:

$$\frac{J_c \times J_c}{\sigma_m} = \sigma_m B_0^2 V^2 \left(\frac{x}{L} y_b\right)\left(\frac{T - T_a}{T_b - T_a}\right). \tag{6}$$

The conduction-radiation energy transfer rate from fin's base is given below

$$q = q_{\text{cond.}} + q_{\text{rad.}} = -k_{\text{eff}}\left(\frac{y_b x}{L}\right)\frac{dT}{dx} - \frac{4\sigma}{3\beta_R}\left(\frac{y_b x}{L}\right)\frac{dT^4}{dx} \tag{7}$$

using $T^4 \approx 4T_a^3 T - 3T_a^4$ and employing the nondimensional terms, the energy Eq. (5) can be rewritten as follows:

$$\begin{aligned}&\frac{d}{dX}\left(X\frac{d\theta}{dX}\right) + \frac{G}{(1+4R_d)}X\theta^{\varepsilon_G} = 2\lambda(X+\omega)\sqrt{1+\psi^2}\frac{Z_0^2(1-\varphi)}{(1+4R_d)}\theta^{n+1} + 2\lambda(X+\omega)\sqrt{1+\psi^2}\frac{R_a}{(1+4R_d)}\theta^2\\ &+2\lambda(X+\omega)\sqrt{1+\psi^2}\frac{R_2}{(1+4R_d)} + X\frac{H_a}{(1+4R_d)}\end{aligned} \tag{8}$$

The following boundary conditions are required to solve the above equations:

$$At\ tip\ :\qquad \theta(X)]_{X=0} = 0 \tag{9a}$$

$$At\ base\ :\quad \theta(X)]_{X=1} = 1 \tag{9b}$$

$$\begin{aligned}&\frac{d^2\theta}{dX^2} + \frac{1}{X}\frac{d\theta}{dX} = -\frac{G}{(1+4R_d)}\theta^{\varepsilon_G} + \frac{2\lambda\sqrt{1+\psi^2}}{(1+4R_d)}Z_0^2(1-\varphi)\theta^{n+1} + \frac{2\lambda\sqrt{1+\psi^2}}{(1+4R_d)}\omega Z_0^2(1-\varphi)\left(\frac{\theta^{n+1}}{X}\right)\\ &+\frac{2\lambda\sqrt{1+\psi^2}}{(1+4R_d)}R_a\theta^2 + \frac{2\lambda\sqrt{1+\psi^2}}{(1+4R_d)}\omega R_a\left(\frac{\theta^2}{X}\right) + \frac{2\lambda\sqrt{1+\psi^2}}{(1+R_d)}R_2\theta^{B+1} + \frac{2\lambda\sqrt{1+\psi^2}}{(1+4R_d)}\omega R_2\left(\frac{\theta^{B+1}}{X}\right)\\ &+\frac{H_a}{(1+4R_d)}\theta\end{aligned} \tag{10}$$

The above Eq. (10) will be solved by modified ADM. The methodology of MADM is available in literature [27, 28]. According to the MADM, the LHS of the Eq. (10) will form the modified differential operator as follows:

$L_X = X^{-1}\frac{d}{dX}X\frac{d}{dX}(\bullet)$ and it is invertible and therefore its inverse operator can be written as follows:

$$L_X^{-1} = \int_0^X X^{-1}\int_0^X X(\bullet)\,dXdX$$

The Eq. (10) can be written in operator form

$$\begin{aligned}&L_X\theta = -\frac{G}{(1+4R_d)}(NA) + \frac{2\lambda\sqrt{1+\psi^2}}{(1+4R_d)}Z_0^2(1-\varphi)(NB_1) + \frac{2\lambda\sqrt{1+\psi^2}}{(1+4R_d)}\omega Z_0^2(1-\varphi)\left(\frac{NB_2}{X}\right) +\\ &\frac{2\lambda\sqrt{1+\psi^2}}{(1+4R_d)}R_a(NC_1) + \frac{2\lambda\sqrt{1+\psi^2}}{(1+4R_d)}\omega R_a\left(\frac{NC_2}{X}\right) + \frac{2\lambda\sqrt{1+\psi^2}}{(1+4R_d)}R_2(ND_1) + \frac{2\lambda\sqrt{1+\psi^2}}{(1+4R_d)}\omega R_2\left(\frac{ND_2}{X}\right)\\ &+\frac{H_a}{(1+4R_d)}\theta\end{aligned} \tag{11}$$

The non-linear terms are expanded in Adomian polynomials [29] in the manner given below

$$\mathrm{NA} = \theta^{\varepsilon_G} = \sum_0^m A_m;$$
$$A_0 = \theta_0^{\varepsilon_G};$$
$$A_1 = \varepsilon_G \theta_0^{\varepsilon-1}\theta_1;$$
$$\cdots$$

$$\mathrm{NB1} = \mathrm{NB2} = \theta^{n+1} = \sum_0^m B_m;$$
$$B_0 = \theta_0^{n+1};$$
$$B_1 = (n+1)\theta_0^n\theta_1;$$
$$\cdots$$

$$\mathrm{NC1} = \mathrm{NC2} = \theta^2 = \sum_0^m C_m;$$
$$C_0 = \theta_0^2;$$
$$C_1 = 2\theta_0\theta_1;$$
$$\cdots$$

$$\mathrm{ND1} = \mathrm{ND2} = \theta^{B+1} = \sum_0^m D_m;$$
$$D_0 = \theta_0^{B+1};$$
$$D_1 = (B+1)\theta_0^B\theta_1;$$
$$\cdots$$

Multiplying by the inverse operator on both sides of the Eq. (11) and expanding the RHS in Maclaurin series expansion

$$\begin{aligned}\theta = \theta(0) + X\frac{d\theta(0)}{dX} - \frac{G}{(1+4R_d)}L_X^{-1}\left(\sum_0^\alpha A_m\right) + \frac{2\lambda\sqrt{1+\psi^2}}{(1+4R_d)}Z_0^2(1-\varphi)L_X^{-1}\left(\sum_0^\alpha B_m\right)\\ + \frac{2\lambda\sqrt{1+\psi^2}}{(1+4R_d)}\omega Z_0^2(1-\varphi)L_X^{-1}\left(\frac{\sum_0^\alpha B_m}{X}\right) + \frac{2\lambda\sqrt{1+\psi^2}}{(1+4R_d)}R_aL_X^{-1}\left(\sum_0^\alpha C_m\right) +\\ \frac{2\lambda\sqrt{1+\psi^2}}{(1+4R_d)}\omega R_aL_X^{-1}\left(\frac{\sum_0^\alpha C_m}{X}\right) + \frac{2\lambda\sqrt{1+\psi^2}}{(1+4R_d)}R_2L_X^{-1}\left(\sum_0^\alpha D_m\right) + \frac{2\lambda\sqrt{1+\psi^2}}{(1+4R_d)}\omega R_2L_X^{-1}\left(\frac{\sum_0^\alpha D_m}{X}\right)\\ + \frac{H_a}{(1+4R_d)}L_X^{-1}\left(\sum_0^\alpha \theta_m\right)\end{aligned} \tag{12}$$

The first component θ_0 is calculated as below

$$\theta_0 = \theta(0) + X\frac{d\theta(0)}{dX} = C$$

Using the recursive relation next higher order terms are computed as follows:

$$\theta_{m+1} = -\frac{G}{(1+4R_d)}L_X^{-1}\left(\sum_0^\alpha A_m\right) + \frac{2\lambda\sqrt{1+\psi^2}}{(1+4R_d)}Z_0^2(1-\varphi)L_X^{-1}\left(\sum_0^\alpha B_m\right) +$$
$$\frac{2\lambda\sqrt{1+\psi^2}}{(1+4R_d)}\omega Z_0^2(1-\varphi)L_X^{-1}\left(\frac{\sum_0^\alpha B_m}{X}\right) + \frac{2\lambda\sqrt{1+\psi^2}}{(1+4R_d)}R_aL_X^{-1}\left(\sum_0^\alpha C_m\right) +$$
$$\frac{2\lambda\sqrt{1+\psi^2}}{(1+4R_d)}\omega R_aL_X^{-1}\left(\frac{\sum_0^\alpha C_m}{X}\right) + \frac{2\lambda\sqrt{1+\psi^2}}{(1+4R_d)}R_2L_X^{-1}\left(\sum_0^\alpha D_m\right) + \tag{13}$$
$$\frac{2\lambda\sqrt{1+\psi^2}}{(1+4R_d)}\omega R_2L_X^{-1}\left(\frac{\sum_0^\alpha D_m}{X}\right) + \frac{H_a}{(1+4R_d)}L_X^{-1}\left(\sum_0^\alpha \theta_m\right), m \geq 0$$

The second component is calculated as follows:

$$\theta_1 = -\frac{G}{(1+4R_d)}L_X^{-1}(A_0) + \frac{2\lambda\sqrt{1+\psi^2}}{(1+4R_d)}Z_0^2(1-\varphi)L_X^{-1}(B_0) + \frac{2\lambda\sqrt{1+\psi^2}}{(1+4R_d)}\omega Z_0^2(1-\varphi)L_X^{-1}\left(\frac{B_0}{X}\right)$$
$$+\frac{2\lambda\sqrt{1+\psi^2}}{(1+4R_d)}R_aL_X^{-1}(C_0) + \frac{2\lambda\sqrt{1+\psi^2}}{(1+4R_d)}\omega R_aL_X^{-1}\left(\frac{C_0}{X}\right) + \frac{2\lambda\sqrt{1+\psi^2}}{(1+4R_d)}R_2L_X^{-1}(D_0) \tag{14}$$
$$+\frac{2\lambda\sqrt{1+\psi^2}}{(1+4R_d)}\omega R_2L_X^{-1}\left(\frac{D_0}{X}\right) + \frac{H_a}{(1+4R_d)}L_X^{-1}(\theta_0)$$

The third component is calculated as follows:

$$\theta_2 = -\frac{G}{(1+4R_d)}L_X^{-1}(A_1) + \frac{2\lambda\sqrt{1+\psi^2}}{(1+4R_d)}Z_0^2(1-\varphi)L_X^{-1}(B_1) + \frac{2\lambda\sqrt{1+\psi^2}}{(1+4R_d)}\omega Z_0^2(1-\varphi)L_X^{-1}\left(\frac{B_1}{X}\right)$$
$$+\frac{2\lambda\sqrt{1+\psi^2}}{(1+4R_d)}R_aL_X^{-1}(C_1) + \frac{2\lambda\sqrt{1+\psi^2}}{(1+4R_d)}\omega R_aL_X^{-1}\left(\frac{C_1}{X}\right) + \frac{2\lambda\sqrt{1+\psi^2}}{(1+4R_d)}R_2L_X^{-1}(D_1) \tag{15}$$
$$+\frac{2\lambda\sqrt{1+\psi^2}}{(1+4R_d)}\omega R_2L_X^{-1}\left(\frac{D_1}{X}\right) + \frac{H_a}{(1+4R_d)}L_X^{-1}(\theta_1)$$

Therefore, final solution is the summation of three components.

$$\theta = \sum_0^m \theta_m = \theta_0 + \theta_1 + \theta_2 \cdots \tag{16}$$

The actual rate of heat transfer of the porous fin from base to tip can be determined using Fourier's law of heat conduction

$$q_{actual} = \frac{k_{eff}y_b b(T_b - T_a)(1+4R_d)}{L}X\frac{d\theta}{dX}\Big]_{X=0} \tag{17}$$

The maximum heat transfer is possible if its area and perimeter are calculated at base.

$$q_{\max} = -q_0[y_b bL] + h_b(1-\varphi)(T_b - T_a)\left[bL\sqrt{1+\psi^2} + y_bL\right] + \frac{\rho g C_p K\beta(T_b - T_a)^2}{\gamma}\left[bL\sqrt{1+\psi^2} + y_bL\right]$$
$$+4\sigma\varepsilon_s T_a^3(T_b - T_a)\left[bL\sqrt{1+\psi^2} + y_bL\right] + \sigma_m B_0^2 V^2(y_b bL) \tag{18}$$

The efficiency (η) of the triangular porous fin can be obtained by the expression

$$\eta = \frac{q_{actual}}{q_{\max}} \frac{X \left.\frac{d\theta}{dX}\right|_{X=0}}{-\frac{G}{(1+4R_d)} + \frac{Z_0^2(1-\varphi)\left(\sqrt{1+\psi^2}+\lambda\right)}{(1+4R_d)} + \frac{R_a\left(\sqrt{1+\psi^2}+\lambda\right)}{(1+4R_d)} + \frac{R_2\left(\sqrt{1+\psi^2}+\lambda\right)}{(1+4R_d)} + \frac{H_a}{(1+4R_d)}} \tag{19}$$

Results and discussion

The objective here is to observe the simultaneous effect of power law index of the coefficient of heat transfer, internal heat generation, and surface emissivity with externally applied electric and magnetic disturbance of triangular porous fin. The governing equations containing multiple temperature variations of thermo-physical parameters represent a mathematical model with two types of complexities, non-linearity, and singularity. The energy equation containing both types of complexities is solved by the theory of modified Adomian decomposition method (MADM). In order to validate the present results, the governing equations are converted into only singular value equations by putting, $G = \varepsilon_G = n = B = R_d = H_a = R_a = R_2 = \omega = \psi = 0, \lambda = 1, Z_0 = 1.5$ and as shown below:

$$X\frac{d^2\theta}{dX^2} + \frac{d\theta}{dX} = (X + \frac{1}{2})Z_0^2\theta \tag{20}$$

The above equation is solved numerically using FDM and both the results of FDM and MADM are plotted for their comparison as shown in Fig. 2. The energy equation contains 12 thermophysical parameter and higher the value of thermophysical parameters

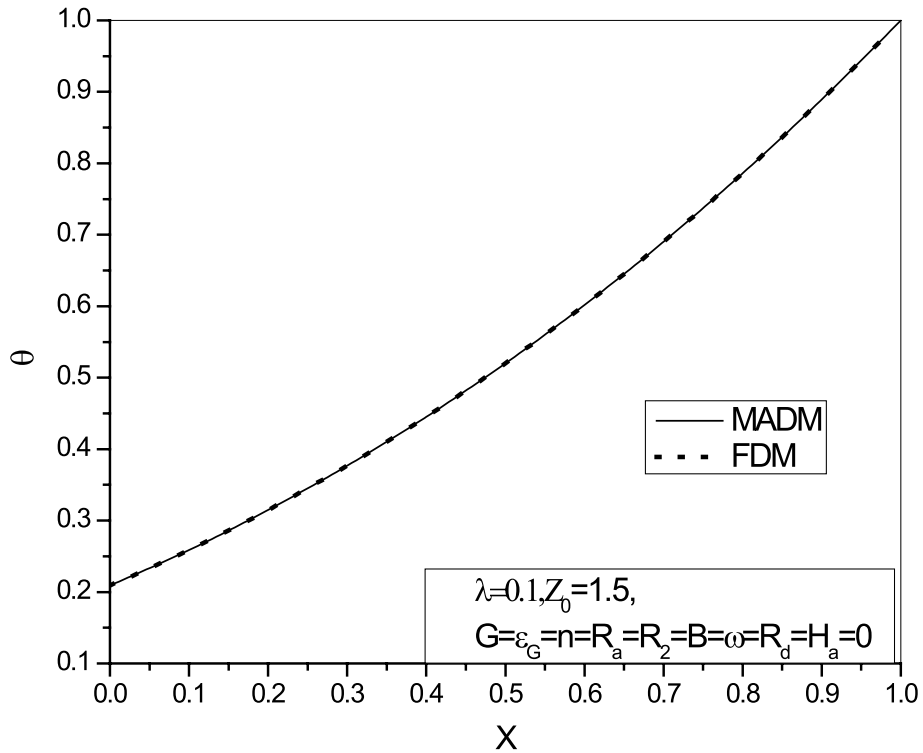

Fig. 2 Comparison of MADM and FDM for the values of Z_0

lead to an increase of absolute error in the fin tip and that may result to an unreliable solution of the problem. For each figure, the power law values are varied simultaneously and kept at same levels. The values of heat generation number and surface ambient radiation parameters are kept at constant and set at low values and other range of parameters for the present problem are as shown in Table 1. Figure 3 exhibits of the effects of combine power index of h, ε, and q, on the temperature curves for the specific values of 0, 0.25, and 0.5, and all the three values are separately exhibited at R_a at 0.001 and 0.1, respectively. The bottom solid and dotted curves represent the tip temperature for constant values of power index parameter i.e., for $\varepsilon_G = n = B = 0$, which implies that heat transfer is not affected at all by combine impact of power index parameters. Top solid and dotted curves indicate highest tip temperature for higher value of power index parameter, i.e., for $\varepsilon_G = n = B = 0.5$ and middle two curves for intermediate values of power index parameter, i.e., for $\varepsilon_G = n = B = 0.25$. It is evident from the figure that the combine effect of power index parameter of convective heat transfer coefficient, internal sources of heat generation, and emissivity parameter of the fin surface amplify the heat transfer process jointly between the working fluids and porous triangular fin. The higher

Table 1 Range of values for physical and thermal parameters

G	$\varepsilon_G = n = B$	R_a	R_2	R_d	H_a	λ	Z_0
0.001	0–0.5	0.001–0.1	0.001	0.001–0.1	0–0.2	0.01–1	1.1–2

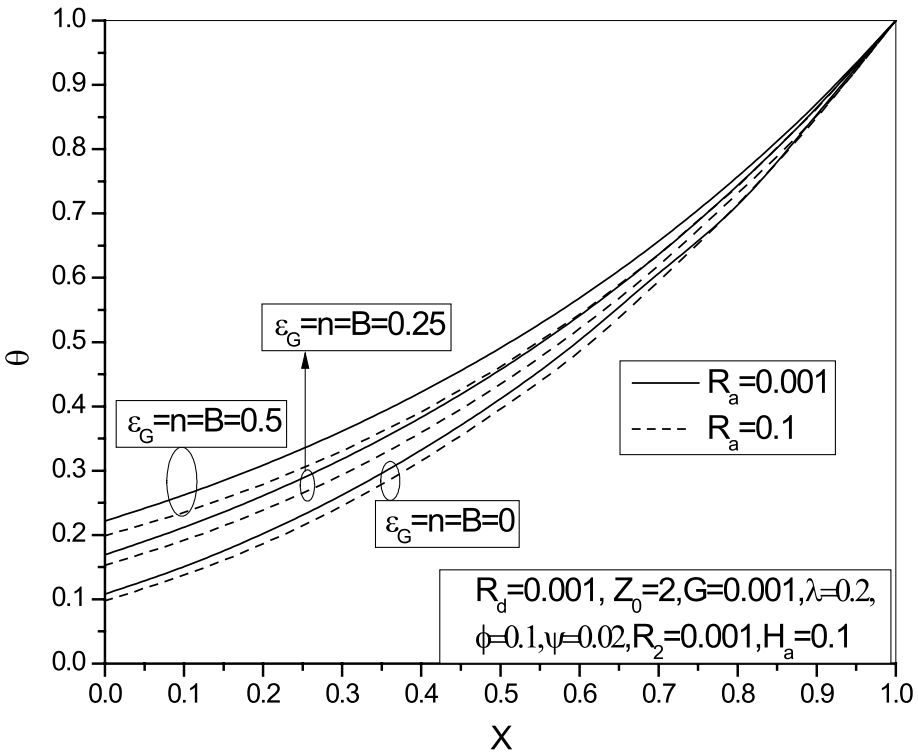

Fig. 3 Effects of combine power index of h,ε, and q, on the temperature curves for the specific values of 0, 0.25, and 0.5 for the values of R_a at 0.001 and 0.1, respectively

value of ε_G, B, and n imposes more nonlinearity in the energy equation and results higher tip temperature and escalate the rate of heat transfer. In addition to the variation of power law, there is a decrease of tip temperature observed, with the increasing value of R_a from 0.001 to 0.1. When R_a increases, it increases the relative permeability of medium to penetrate more fluids which in turn causes to increase of buoyant force in conjunction with the increase of power law parameters. The relative spacing between the solid and dotted line is more for $\varepsilon_G = n = B = 0.5$, which indicates that R_a influences more heat transfer rate for higher value of power law parameters. Figure 4 manifests the tip temperature of the triangular porous fin for three values of H_a at 0, 0.1, and 0.2, and each three values are separately analyzed when R_d at 0.001 and 0.1, respectively. It is assumed that the external magnetic fields influence the working fluids and by virtue of this the working fluids inside the porous fin experience an extra movement for heat transfer. Since H_a indicates the ratio of external magnetic field to the viscous force, the solid curve indicates that tip temperature without any external magnetic field, which means that the fluid particles inside the fin are not affected by the H_a. As the value of H_a increases, it decreases the viscous force and amplifies the buoyancy force for extra movement of the working fluids inside the fin. As a result, the convective heat transfer coefficient of the fluid particles decreases thereby increasing heat conduction mechanism. The thermophysical parameter R_d indicates the combined mode of conduction and radiation from the base of the fin and it is evident that with an increasing value of R_d, tip temperature increases for all values of H_a which implies that R_d influences the external magnetic effect of porous triangular fin. Figure 5 shows the temperature distribution of the triangular porous fin when the values of λ is equal to 0.01, 0.1, and 0.2 and each of

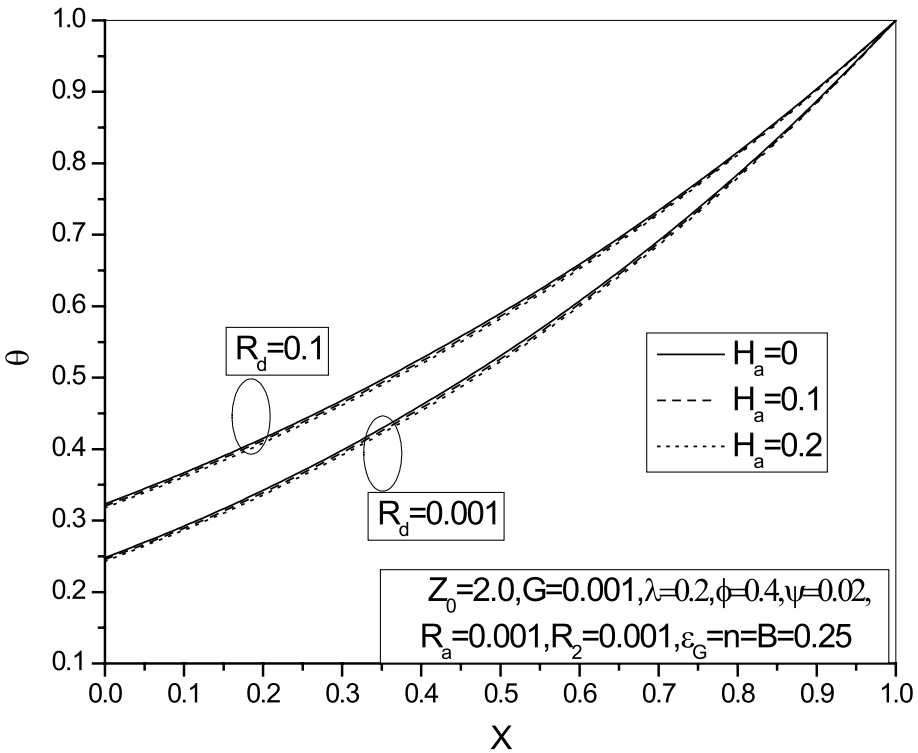

Fig. 4 Effects of H_a on the temperature curves for the values of R_d at 0.001 and 0.1, respectively

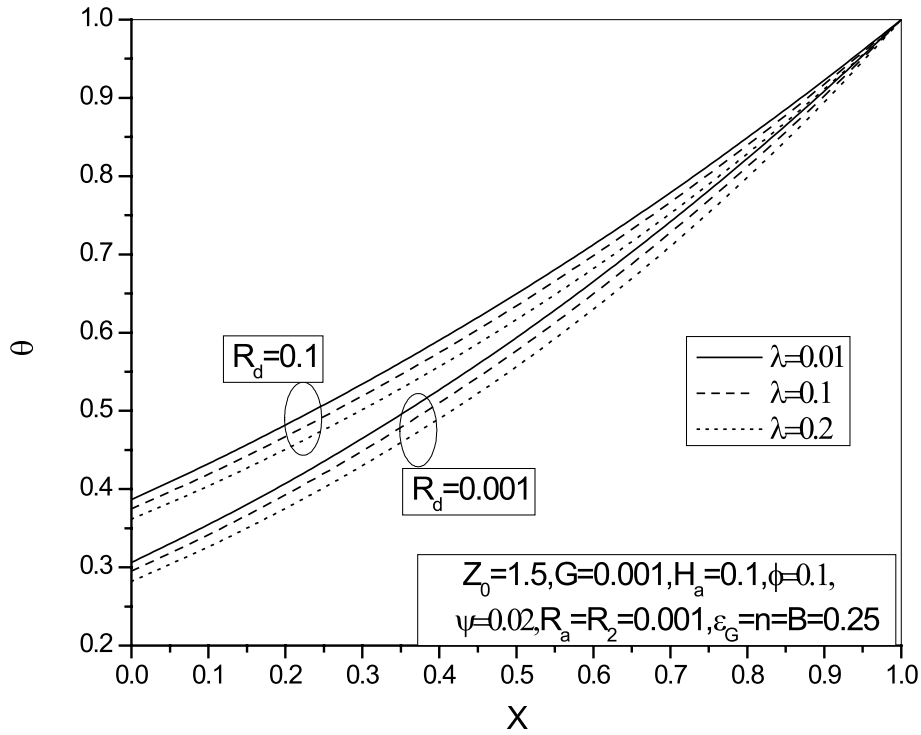

Fig. 5 Effects of λ on the temperature curves when the values of R_d at 0.001 and 0.1, respectively

the three values are further computed when R_d is equal to 0.001 and 0.1, respectively while other parameters are affixed. The λ is the ratio of half fin thickness at the base to the lateral thickness of the triangular porous fin and it is the important design parameter that defines the relationship between the vertical height at the base with respect to the width of the triangular porous fin. Tip temperature is highest for $\lambda = 0.01$ and as the value of λ increases, the temperature curves have a tendency to sag downwards, which means that higher value of λ provides more non-linearity effect in the energy equation. Therefore, it concludes in other way that wider triangular porous fin leads to a higher tip temperature because of the increased surface area. Further, it is evident from the figure that the higher value of R_d increases the tip temperature for all values of λ. Figure 6 depicts the combined impact of ε_G, B, and n, on the tip temperature of porous triangular fin when the values of ψ are at 0 and 0.4, respectively. The parameter ψ is the ratio of half fin thickness at the base with respect to the length and it is important design parameter that defines the vertical height at the base to the length of the triangular porous fin. The value of ψ indicates the specification in vertical plane and when $\psi = 0$, it represents zero slope in vertical plane. It is evident from the figure that the tip temperature is highest when $\psi = 0$ and as the value ψ increases, the tip temperature decreases and its effect remain constant with increase or decrease of the power law parameters. Figure 7 shows the variation of value of η , with respect to φ for the different values of H_a. The left-hand side of the graph represents efficiency of the solid fin since the value of φ is zero. As the value of φ increases, it provides an extra surface area by removing solid material and increases heat convection and increases the efficiency. The fin efficiency is lowest without any external magnetic field and it was represented by the dotted lines for $H_a = 0$ as

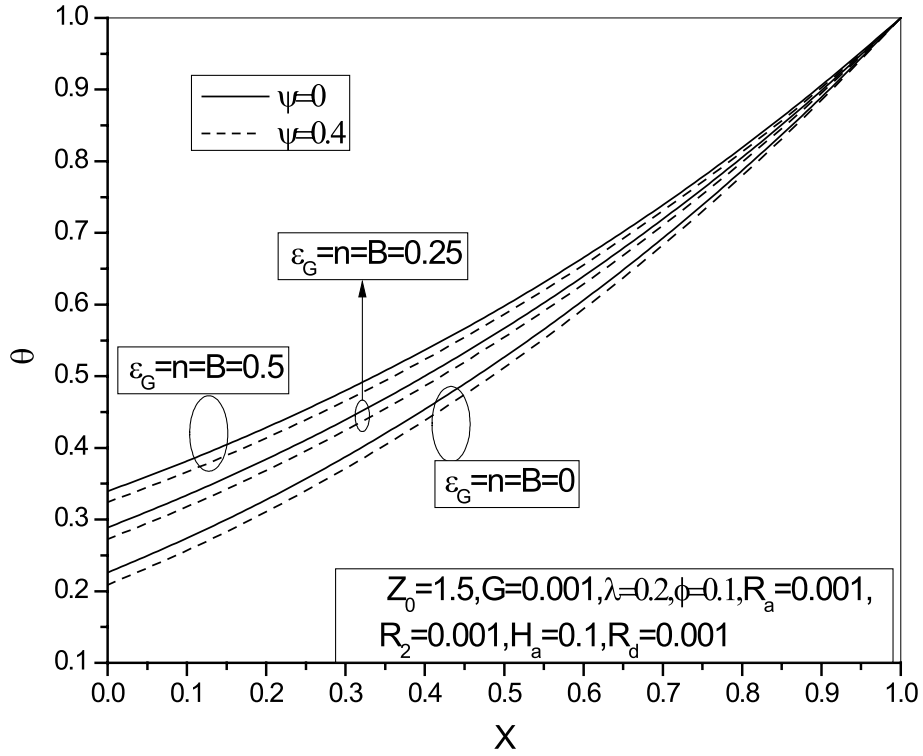

Fig. 6 Effects combine power index of *h*,*ε*, and *q* on the tip temperature of porous triangular fin when the values of ψ at 0 and 0.4, respectively

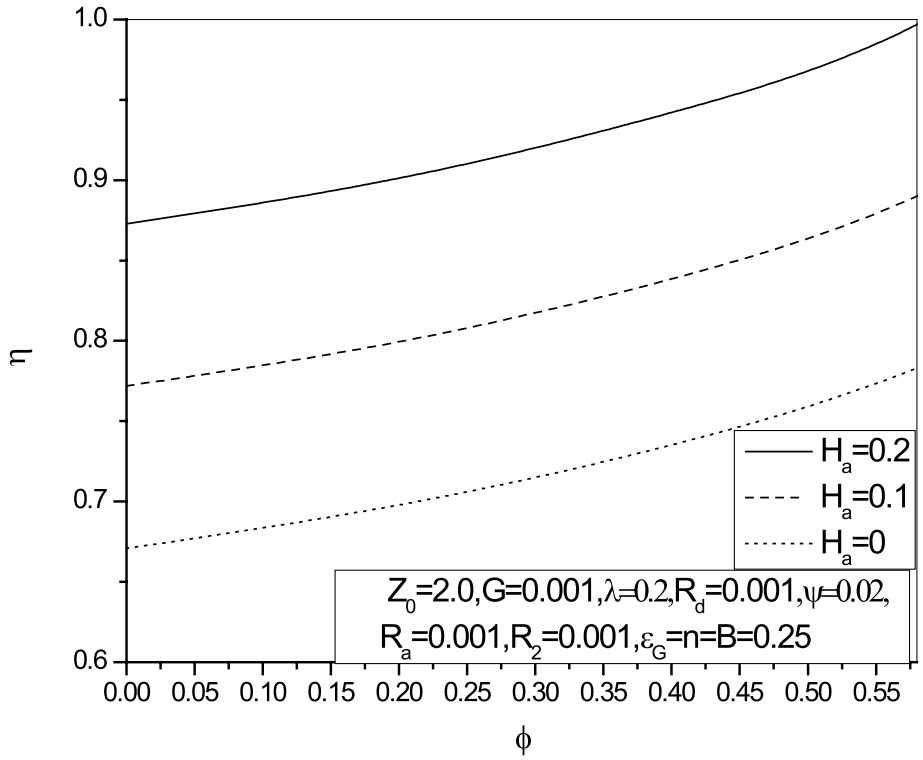

Fig. 7 Effect of η with respect to φ for the different values of H_a

shown in the figure. When both the values of H_a and φ increases, η increases rapidly. The increased surface area increases the heat convection of the fluid particles in the passage and simultaneously the application of external magnetic field increases heat conduction in solid matrices and that ultimately leads to higher η. Figure 8 shows variation of η, with respect value of Z_0 when power index parameters ε_G, n, B are equal to 0, 0.25, and 0.5, respectively. It has been found that the fin efficiency is highest when power index parameters of q, ε, and h is equal to 0 and increasing the value of power index parameters, the fin efficiency decreases. Also, the fin efficiency has decreasing trends with the increase of value Z_0. Figure 9 depicts the variation of η, with respect value to λ for values of R_a equal to 0.001 and 0.1 and effect of R_a are further displayed when the values of φ is equal to 0.1 and 0.2, respectively. It is evident from the figure that, for higher value of φ, the higher is the fin efficiency and also the efficiency curves have increased value when R_a is equal to 0.1. All the curves have an increasing trend with the increase of λ. Figure 10 depicts the variation of η, with respect value to ψ for the values of ε_G, n, B equal to 0, 0.25, and 0.5 while other parameters at fixed level. It has been found that the fin efficiency is highest when power index parameters of q, ε, and h are equal to 0 and increasing value of power index parameters, the fin efficiency have decreasing trends with increase of ψ.

Conclusions

In the present study, simultaneous variation of power law-dependent heat transfer coefficient, internal heat generation, and surface emissivity parameters under the influence of external magnetic and electric fields of triangular porous fin were analyzed using modified Adomian decomposition method (MADM) and then results of MADM had

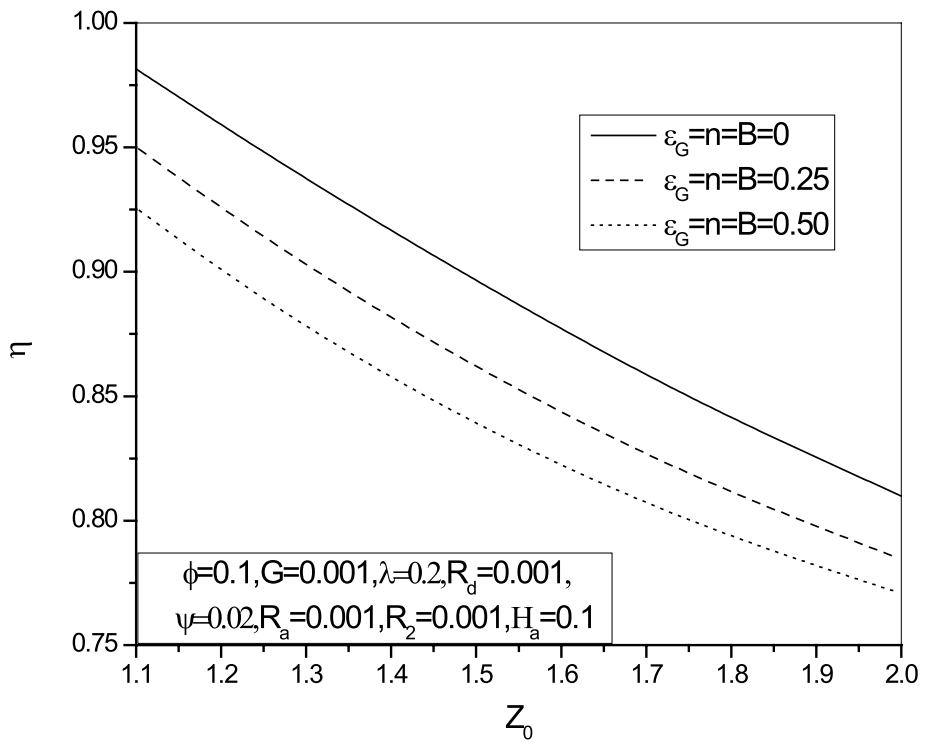

Fig. 8 Effects of η with respect value of Z_0 for different values of power index parameters

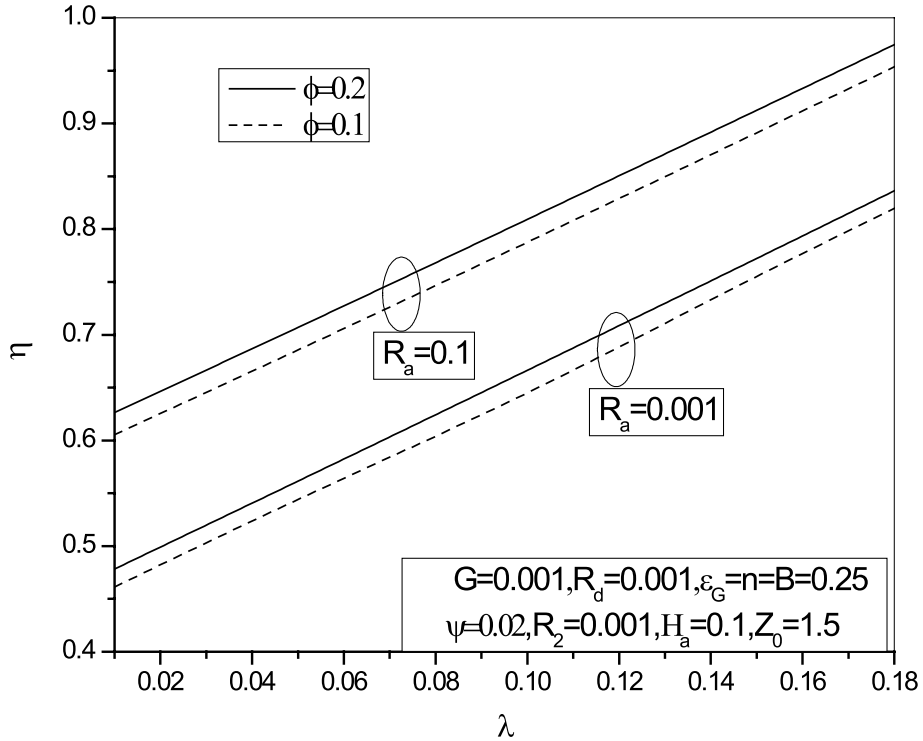

Fig. 9 Effect of η with respect value to λ for values of R_a equal to 0.001 and 0.1, respectively

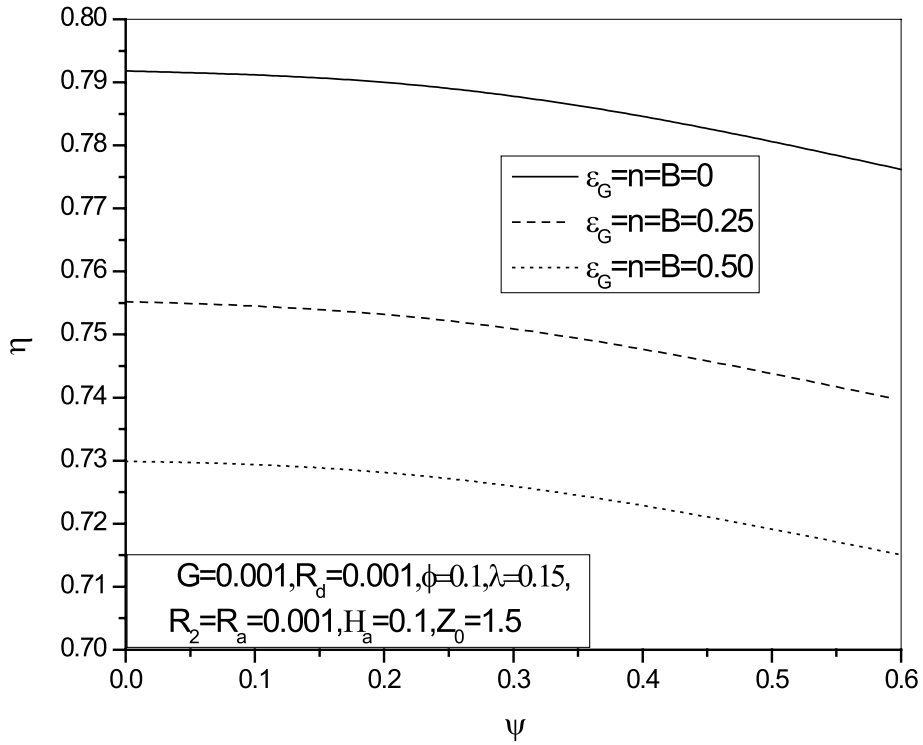

Fig. 10 Effect of η with respect value to ψ for different values of power index parameters

been compared with FDM in the limiting condition and it had been observed that both the results were in good agreement. The comparative study was carried out between significant parameters like multiple power law parameters, Hartmann number at zero and non-zero values while other pertinent thermophysical parameters like modified Rayleigh number, radiation-conduction parameter, surface ambient-radiation parameter and two important fin design parameters like, half fin thickness at the base to length and base to width had been varied and discussed graphically. It had been found that with the increased values of the combined power law-dependent parameter, the higher the tip temperature of the porous triangular fin ultimately enhanced the rate of heat transfer between the working fluid and porous fin. It was also observed that the tip temperature of the porous triangular fin was decreasing trends when the Hartmann number was increasing and also with the decreasing trends of radiation conduction parameters. Further, it was evident from the design parameters that the wider triangular porous fin had a higher tip temperature and higher heat transfer rate. From this study, it had been found that with the increasing value of Hartmann number, porosity parameter as well as half thickness at the base to width parameter, the efficiency of the triangular porous fin was increasing rapidly and the efficiency of the porous fin was highest when power law parameters were kept at a constant value and also the efficiency was decreasing trends when fin parameter was increasing.

The MADM also can be applied for solving longitudinal triangular wet fin with multiple power law-dependent thermal parameters with insulated boundary conditions as a scope of future work. Similarly, same MADM can be applied for convex wet fins or any longitudinal fins whose thickness changes from base to tip both linearly and non-linearly with insulated boundary conditions.

Nomenclature

K Thermal conductivity, $\frac{W}{m.K}$
$T(x)$ Temperature function of fin length, K
P_x Perimeter at location x, m
T_b Dimensional temperature at the base, K
T_a Temperature at ambient condition, K
$q(T)$ Internal heat generation power function of (T,T_a,T_b), $\frac{W}{m^3}$
$h(T)$ Heat transfer co-efficient, $\frac{W}{m^2.K}$
n,B,ε_G Power exponent
R_a Modified form of Rayleigh number, $\frac{gKb(T_b-T_a)L}{agk_Ry}$,
R_d Radiation-conduction parameter, $\frac{4\sigma T_a^3}{3k_{\text{eff}}\beta_R}$
R_2 Surface ambient-radiation parameter, $R_2=\frac{4\sigma\varepsilon_s T_a^3 L}{k_{\text{eff}}\psi}$
H_a Hartmann number, $\frac{\sigma_m B_0^2 V^2 L^2}{k_{\text{eff}}(T_b-T_a)}$
Z_0 Fin parameter, $\sqrt{\frac{h_b L^2}{k_{\text{eff}} y_b}}$
G Heat generation number, $\frac{q_0 L^2}{k_{\text{eff}}(T_b-T_a)}$
k_R Thermal conductivity ratio, $\frac{k_{\text{eff}}}{k_f}$
X Axial coordinate measured from fin tip, m
Y Vertical coordinate measured from fin tip, m
A_x Cross-section at the location x, m^2

X Dimensionless coordinate measured from fin tip, $\frac{x}{L}$
J_c Conduction current density, $\frac{A}{m}$
E External electric field
B_0 Magnetic field, Tesla
V_w Darchy velocity, $\frac{m}{s}$
V Macroscopic velocity of fluid due to electric and magnetic field, $\frac{m}{s}$
C_p Specific heat, $\frac{J}{kg.K}$
b Width, m
t_b Thickness at the base, m
E Electrical field, $\frac{V}{m}$
$\varepsilon(T)$ Surface emissivity of power function of (T,T_a,T_b),
ψ Half fin thickness measured at the base to length ratio, $\frac{y_b}{L}$
λ Half fin thickness measured at the base to width in dimensionless form, $\frac{y_b}{b}$
φ Parameter denote porosity
θ Temperature in dimensionless form, $\frac{T-T_a}{T_b-T_a}$
ε_s Emissivity parameter of surface w.r.t. atmosphere
σ Stephen–Boltzmann constant, $\frac{W}{m^2.K^4}$
γ Kinematic viscosity, $\frac{m^2}{s}$
α Thermal diffusivity, $\frac{k_f}{\rho C_p}$
ρ Fluid density, $\frac{\mathrm{kg}}{\mathrm{m}^3}$
β Thermal expansion co-efficient, $\frac{1}{K}$
$\omega\frac{1}{2\lambda}$
σ_m Electrical conductivity, $\frac{A}{m}$
β_R Mean absorption coefficient of Rossland

Abbreviations

MADM	Modified Adomian decomposition method
FDM	Finite difference method
DTM	Differential transform method
CM	Collocation method
LSM	Least square method
DJM	Daftardar–Gejiji and Jafari method
ADM	Classical Adomian decomposition method

Acknowledgements
Not applicable.

Authors' contributions
Pranab Kanti Roy, corresponding author of the paper contributed the idea of the paper and wrote the whole manuscript. Joy Prakash Das, the co-author of the paper helped to generate the number of components of MADM as well as FDM and also to implements Newton's Rapson method. Both of us read and approved the manuscript.

Funding
The authors declare that they have no funding for the research.

Availability of data and materials
Data sharing is not applicable to this article as no datasets were generated or analyzed during the current study.

Declarations

Competing interests
The authors declare that they have no competing interests.

Received: 13 July 2023 Accepted: 15 September 2023
Published online: 28 September 2023

References

1. Poulikakos D, Bejan A (1982) Fin geometry for minimum entropy generation in forced convection. J Heat Transfer 104:616–623. https://doi.org/10.1115/1.3245176
2. Shekarriz A, Plumb OA (1989) Enhancement of film condensation using porous fins. J Thermophys Heat Transfer 3(3):309–314. https://doi.org/10.2514/3.28777
3. Kim SY, Paek JW, Kang BH (2000) Flow and heat transfer correlations for porous fin in a plate-fin heat exchanger. J Heat Transfer 122(3):572–578. https://doi.org/10.1115/1.1287170
4. Kem DQ, Kraus DA (1972) Extended surface heat transfer. McGraw–Hill, New York
5. Vaszi AZ, Elliott L, Ingham DB, Pop I (2004) Conjugate free convection from a vertical plate fin with a rounded tip embedded in a porous medium. Int J Heat Mass Transf 47(12–13):2785–2794. https://doi.org/10.1016/j.ijheatmasstransfer.2004.01.001
6. Kiwan S, Zeitoun O (2008) Natural convection in a horizontal cylindrical annulus using porous fins. Int J Numer Meth Heat Fluid Flow 18(5):618–634. https://doi.org/10.1108/09615530810879747
7. Kiwan S, Al-Nimr MA (2001) Using porous fins for heat transfer enhancement. J Heat Transfer 123(4):790–795. https://doi.org/10.1115/1.1371922
8. Kiwan S (2006) Thermal analysis of natural convection in porous fins. Transp Porous Media 67:17–29. https://doi.org/10.1007/s11242-006-0010-3
9. Gorla RSR, Bakier AY (2011) Thermal analysis of natural convection and radiation in porous fins. Int Commun Heat Mass Transf 38(5):638–645. https://doi.org/10.1016/j.icheatmasstransfer.2010.12.024
10. Kundu B, Bhanja D (2011) An analytical prediction for performance and optimum design analysis of porous fins. Int J Refrig 34:337–352. https://doi.org/10.1016/j.ijrefrig.2010.06.011
11. Kundu B, Bhanja D (2011) Thermal analysis of a construal T-shaped porous fin with radiation effects. Int J Refrig 34:1483–1496. https://doi.org/10.1016/j.ijrefrig.2011.04.003
12. Moradi A, Hayat T, Alsaedi A (2014) Convection-radiation thermal analysis of triangular porous fins with temperature dependent thermal conductivity by DTM. Energy Convers Manage 77:70–77. https://doi.org/10.1016/j.enconman.2013.09.016
13. Hatami M, Hasanpour A, Ganji DD (2013) Heat transfer study through porous fins (Si_3N_4 and AL) with temperature-dependent heat generation. Energy Convers Manage 74:9–16. https://doi.org/10.1016/j.enconman.2013.04.034
14. Oguntala G, Sobamowo G, Abd-Alhameed R, Jones S (2019) Efficient iterative method for investigation of convective–radiative porous fin with internal heat generation under a uniform magnetic field. Int J Appl Comput Math 5:13. https://doi.org/10.1007/s40819-022-01369-3
15. Roy PK, Mallick A, Mondal H, Goqo S, Sibanda P (2017) Numerical study on rectangular-convex-triangular profiles with all variable thermal properties. Int J Mech Sci 133:251–259. https://doi.org/10.1016/j.ijmecsci.2017.07.066
16. Roy PK (2022) A decomposition solution of variable thickness absorber plate solar collectors with power law dependent thermal conductivity. J Therm Sci Eng Appl 14(8):084501. https://doi.org/10.1115/1.4053118
17. Mosayebidorcheh S, Ganji DD, Farzinpoor M (2014) Approximate solution of the nonlinear heat transfer equation of a fin with power law temperature dependent thermal conductivity and heat transfer co-efficient. Propuls Power Res 3(1):41–47. https://doi.org/10.1016/j.jppr.2014.01.005
18. Moitsheki RJ, Hayat T, Malik MY (2010) Some exact solutions of the fin problem with a power law temperature-dependent thermal conductivity. Nonlinear Anal Real World Appl 11(5):3287–3294. https://doi.org/10.1016/j.nonrwa.2009.11.021
19. Moitsheki RJ (2011) Steady one-dimensional heat flow in a longitudinal triangular and parabolic fin. Commun Nonlinear Sci Numer Simul 16:3971–3980. https://doi.org/10.1016/j.cnsns.2011.01.010
20. Sobamowo MG, Alaribe KC, Adeleye AO (2020) A study on the impact of lorentz force on the thermal behaviour of a convective-radiative porous fin using differential transformation method. Int J Mech Dyn Anal 6:45–58
21. Das R, Kundu B (2021) Predicting of heat generation and electromagnetic parameters from temperature response in porous fin. J Thermophys Heat Transf 6:45–58. https://doi.org/10.2514/1.T6224
22. Hoshyar HA, Ganji DD, Majidian AR (2016) Least square method for porous fin in the presence of uniform magnetic field. J Appl Fluid Mech 9(2):661–668. https://doi.org/10.18869/acadpub.jafm.68.225.24245
23. Patel T, Meher R (2017) Thermal analysis of porous fin with uniform magnetic field using Adomian decomposition Sumudu transforms method. Nonlinear Eng 6(3):1–10. https://doi.org/10.1515/nleng-2017-0021
24. Gireesha BJ, Sowmya G, Srikantha N (2022) Heat transfer in a radial porous fin in the presence of magnetic field: a numerical study. Int J Ambient Energy 43(1):3402–3409. https://doi.org/10.1080/01430750.2020.1831599
25. Madhura KR, Babitha, Kalpana G, Makinde OD (2020) Thermal performance of straight porous fin with variable thermal conductivity under magnetic field and radiation effects. Heat Transf 49(8):5002–2019. https://doi.org/10.1002/htj.21864
26. Das R, Kundu B (2021) An estimate of heat generation, electric, and magnetic parameters from temperature fields in porous fins for electronic cooling system. IEEE Trans Compon Packag Manuf Technol 11(8):1250–1257. https://doi.org/10.1109/TCPMT.2021.3099062
27. Adomian G (1994) Solving frontier problems in physics: the decomposition method. Kluwer Academic Publishers, Dordrecht
28. Roy PK, Mallick A, Mondal H, Sibanda P (2018) A modified decomposition solution of triangular moving fin with multiple variable thermal properties. Arab J Sci Eng 43:1485–1497. https://doi.org/10.1007/s13369-017-2983-3
29. Roy PK, Mondal H, Raj B. Analytical and numerical solution of the longitudinal porous fin with multiple power-law-dependent thermal properties and magnetic effects. Heat Transf. 2021:1–21. https://doi.org/10.1002/htj.22421.

Publisher's Note